Article

Not peer-reviewed version

Improving Pure Titanium's Biological and Mechanical Characteristics through ECAP and Micro Arc Oxidation Processes

Dawit Bogale Alemayehu , Masahiro Todoh , J. H. Hsieh , Chuan Li , Song-Jeng Huang *

Posted Date: 2 June 2023

doi: 10.20944/preprints202306.0173.v1

Keywords: Pulp cell; Periodontal cell; Micro-Arc Oxidation (MAO), Sever Plastic deformation (SPD), Equal Channel Angular Pressing (ECAP), AlamarBlue; ELISA; trypsin

Article

Improving Pure Titanium's Biological and Mechanical Characteristics through ECAP and Micro Arc Oxidation Processes

Dawit Bogale Alemayehu [1], Masahiro Todoh [2], J. H. Hsieh [3], Chuan Li [4,5] and Song-Jeng Huang [6,*]

[1] Division of Human Mechanical Systems and Design, Graduate School of Engineering, Hokkaido University, Sapporo 060-8628, Japan; zetseatdawit2018@gmail.com
[2] Division of Mechanical and Aerospace Engineering, Faculty of Engineering, Hokkaido University, Sapporo 060-8628, Japan; todoh@eng.hokudai.ac.jp
[3] Department of Materials Engineering, Ming Chi University of Technology, Taishan, Taipei 24301, Taiwan
[4] Department of Biomedical Engineering, National Yang Ming Chiao Tung University, Taipei 11221, Taiwan
[5] Department of Mechanical Engineering, National Central University, Jhongli, Taoyuan 32001, Taiwan
[6] Department of Mechanical Engineering, National Taiwan University of Science and Technology, Taipei 106, Taiwan
* Correspondence: sgjghuang@mail.ntust.edu.tw

Abstract: Pure titanium is limited to be used in biomedical applications due to its lower mechanical strength compared to its alloy counterpart. To enhance its properties and improve medical implants feasibility, advancements in titanium processing technologies are necessary. One such technique is equal channel angular pressing (ECAP) for its severe plastic deformation (SPD). This study aimed to surface modify commercially pure titanium using micro arc oxidation (MAO) technology and mineral solutions containing Ca and P. The composition and shape of the changed surface were characterized using X-ray diffraction (XRD) and scanning electron microscope (SEM), respectively. The weight % of Ca and P in the coating was determined using Energy Dispersive Spectroscopy (EDS), and the corrosion resistance was evaluated through potentiodynamic measurement. The behavior of human dental pulp cell and periodontal cell behavior was also studied through a biomedical experiment over a period of 1-, 3-, and 7-days using trypsin as the culture medium and ELISA as the observation method. This study showed that the mechanical grain refinement method and surface modification significantly improved the biomechanical properties of commercially pure (CP) Titanium. Although the results showed variations in the absorbance values of cells cultured on different surfaces, this study provides valuable insights into pulp cell behavior and advances the field of biomedical research.

Keywords: pulp cell; periodontal cell; micro-arc oxidation (MAO); sever plastic deformation (SPD); equal channel angular pressing (ECAP); AlamarBlue; ELISA; trypsin

1. Introduction

In recent years, the field of medical implants has made remarkable strides, rapidly becoming a crucial component of modern healthcare [1]. The biomedical industry makes extensive use of commercially pure (CP) Ti and related alloys due to their biocompatibility, corrosion resistance, and mechanical characteristics [2,3,12]. Even though they are biocompatible, their lower mechanical strength compared to titanium alloys precludes their use in load-bearing implants [13–15]. To combat this, researchers are attempting to enhance the mechanical properties of CP Ti, including its strength, ductility, and fatigue resistance [12,16–19]. Besides, improving biocompatibility is crucial, which can be achieved through surface modification [20–22] or tailoring the composition with bioactive elements such as calcium, phosphorus, and oxygen [23–26]. Therefore, Improving the mechanical

 doi:10.20944/preprints202306.0173.v1

properties and biocompatibility of CP Ti through continuous research is essential for the development of safe and effective biomedical implants.

Severe plastic deformation (SPD) techniques, specifically equal channel angular pressing (ECA P, are advantageous for improving the mechanical properties of CP Ti [27–29]. Because of their potential to enhance the mechanical characteristics of metals, these technologies have attracted a lot of interest in the field of material science. ECAP, a prominent SPD technique that has been shown to substantially increase both strength and ductility, can be used to refine the particle size of multiple metals, including CP Ti [30,31]. During the ECAP process, an extremely severe plastic deformation is induced in the billet by passing it through an angular channel die [27,32,33]. During this process, the particle size of the material decreases significantly, which increases its strength and ductility [30]. In conclusion, ECAP is an effective method for enhancing the mechanical properties of CP Ti. This procedure considerably increases the material's strength and ductility by reducing the particle size and generating a uniform microstructure composed of ultrafine grains. ECAP has shown promise in the past as a technique for improving the mechanical properties of CP Ti for use in a variety of applications, including medical implants and aerospace components [34].

Surface behaviors of CP Ti are equally as essential as its mechanical properties when assessing the biological function of implants [35,36]. The surface of CP Ti has been modified using techniques such as micro arc oxidation (MAO) in order to increase its bioactivity and biocompatibility [37,38]. It has been reported that MAO forms a porous and bioactive coating on CP Ti by incorporating calcium (Ca) and phosphorus (P), which are known to promote bone integration [39,40]. MAO-treated CP Ti exhibits enhanced corrosion resistance, cell adhesion, proliferation, and differentiation [41–45].

Combining ECAP and MAO has been suggested to improve the mechanical and surface characteristics of CP Ti for biomedical applications [16,46–50]. However, Little research has been conducted on how the integration of these approaches influences the biological efficacy of CP Ti, specifically pulp cell activity. The biocompatibility of implant materials, such as CP Ti, has been investigated using human dental pulp cells in cell culture [51,52]. Using enzyme-linked immunosorbent assay (ELISA) as a monitoring instrument, trypsin may be utilized to assess cell viability and proliferation on a variety of surfaces [53].

This study's primary objective is to determine how the biomechanical properties of CP Ti influence the activity of ECAP- and MAO-treated human dental pulp cells and periodontal cells. In addition, ECAP and MAO are predicted to enhance the mechanical and surface properties of CP Ti. After ECAP and MAO treatment, the mechanical and surface properties of CP Ti should improve, resulting in enhanced corrosion resistance behavior, proliferation and differentiation of human dental pulp and periodontal cells.

2. Materials and Methods

2.1. Equal Channel Angular Pressing (ECAP) Process

Commercially pure grade 4 pure titanium long strips purchase from a local supplier (President Co., Ltd., Taiwan) were processed by the equal channel angular pressing (ECAP) as shown schematically in **Figure 1**. The ECAP belongs to the class of sever plastic deformation (SPD) processes, which aim to produce ultra fine grains (UFG) in materials to enhance their mechanical strength. Note that in **Figure 1**, the angle of intersection between the channels and the exit is 120° and the processing temperature is set at 400°C. Each workpiece went through the process twice. At the end of each process, the workpiece was rotated 90° about its longitudinal axis (y) to ensure uniform deformation achieved in materials. In addition, the same material without ECAP (0 pass) is also studied as a control group for all tests in this study.

Preprints.org (www.preprints.org) | NOT PEER-REVIEWED | Posted: 2 June 2023 doi:10.20944/preprints202306.0173.v1

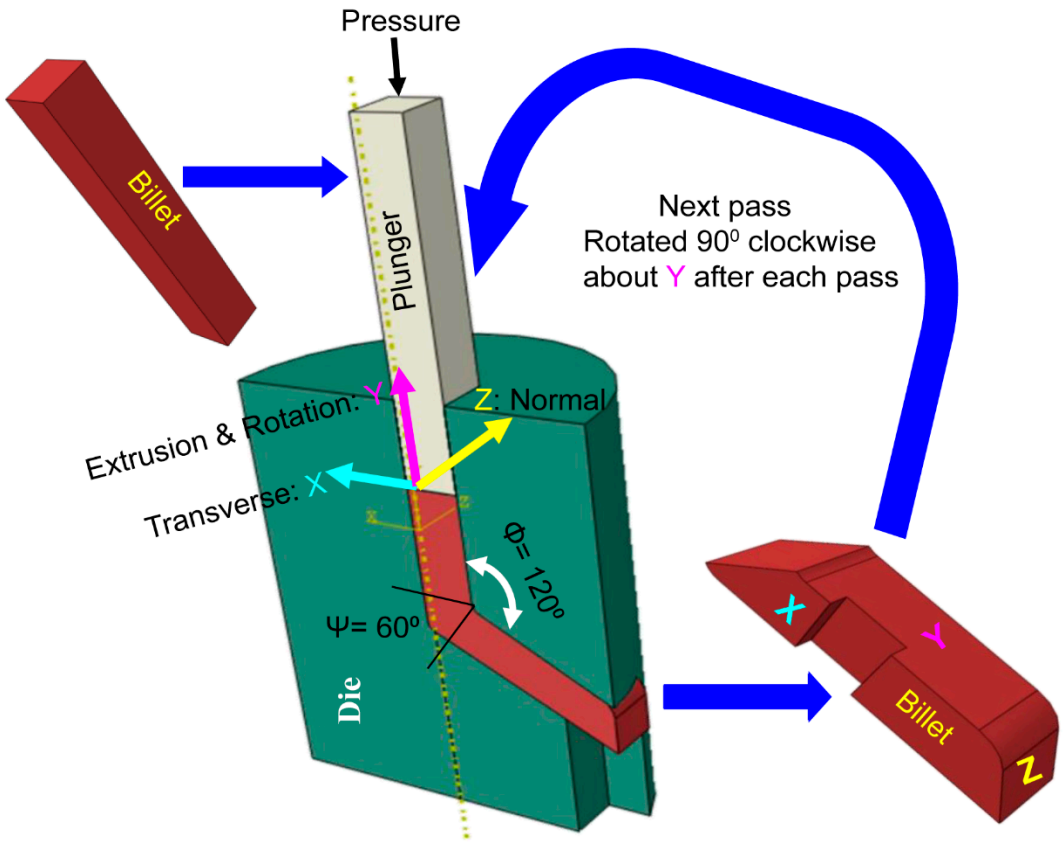

Figure 1. Design and process of the ECAP for grade 4 pure titanium strips.

For a given N number of pass of polycrystalline metals subjected to side extrusion, a total of the induced equivalent plastic strain can be calculated as follows [30]:

$$\varepsilon_T = \frac{N}{\sqrt{3}}\left(2\,cot\left(\frac{\emptyset}{2}+\frac{\Psi}{2}\right)+\Psi\,cosec\left(\frac{\emptyset}{2}+\frac{\Psi}{2}\right)\right) \quad (1)$$

Where Ψ is the arc of curvature and $\emptyset$ is the intersection angle, as depicted in **Figure 1**.

2.2. Micro Arc Oxidation (MAO) Coating

After ECAP process, we cut workpieces into small specimens of 45 × 9 × 9 mm^3. The specimen was mechanically polished by 240, 400, 600, 800, 1000, 1500 and 2000 SiC abrasive papers in turn, followed by cleaning with alcohol and deionized water, and finally dried in air before coating. The coating is implemented by electrochemically using micro-arc oxidation (MAO) as depicted in **Figure 2A and 2B**. The specimen is placed at anode, while a stainless-steel wall of container is used as cathode. The aqueous electrolyte are 4.203 g/L Calcium glycerophosphate hydrate ($C_7H_7CaO_6P$-$2H_2O$), 23.72 g/L of calcium acetate ($Ca(CH_3COO)$-$2H_2O$), and 4 g/L of EDTA-Na (Ethylene Diamine Tetra Acetic Acid) ($C_{10}H_{16}N_2O_8$). The coating lasted for 20 min at a constant current density of 1.6 A/dm^2. The duty cycle, voltage at anode and frequency are 20%, 320 V and 50 Hz respectively. To maintain an isothermal condition during MAO, the steel container was cooled in water cycling continuously during the whole process.

Preprints.org (www.preprints.org) | NOT PEER-REVIEWED | Posted: 2 June 2023 doi:10.20944/preprints202306.0173.v1

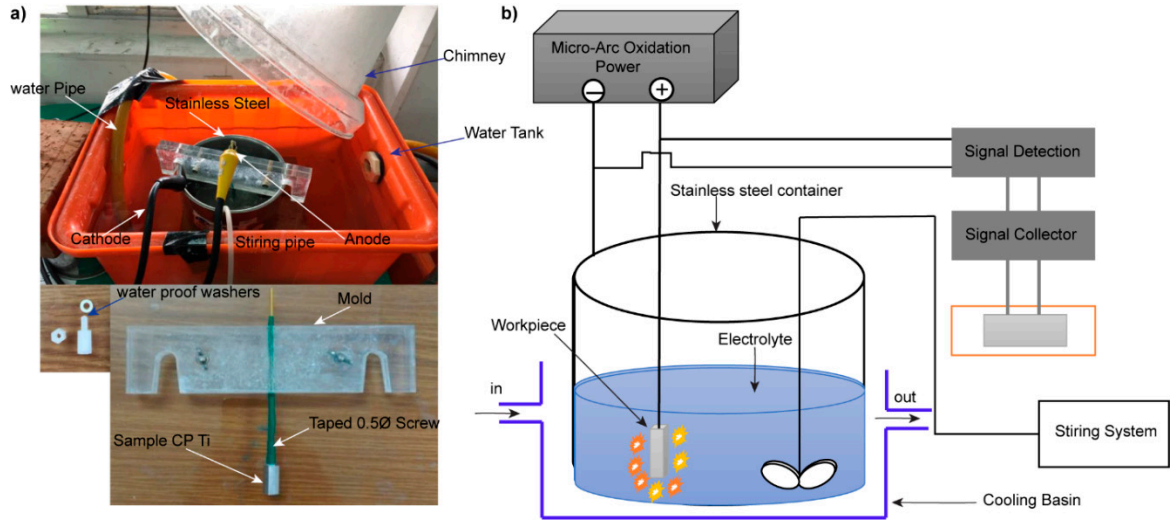

Figure 2. Schematic representation of A) the micro-arc oxidation (MAO) setup and B) coating Technology.

3.2. Electrochemical Test

Ti is highly resistant to corrosion due to its self-passivation. To determine the basic properties of corrosion resistance, two electrochemical tests were conducted – potentiodynamic test for determining the open circuit potential (OCP) from polarization curve and electrochemical impedance spectroscopy (EIS) using the Nyquist Plot.

For the potentiodynamic test (Versastat-3, Princeton Applied Research, USA), the three-electrode scheme depicted in **Figure 3** was used to determine the polarization curves. The reference electrode is Ag/AgCl/KCl, the auxiliary electrode is carbon black, and the working electrode is the Ti sample. The samples were polished with abrasive papers of decreasing grit size and a diamond paste. Then they were degreased with white spirit solution (mixture of aliphatic, open chain or alicyclic C7 to C12 hydrocarbons) and installed into the three-electrode potentiodynamic system. The electrolyte is a mixture of ~3.5 wt. % (36.5 g/1.0 l deionized H_2O) NaCl solution at 37°C. Before potentiodynamic test, the open circuit potential (OCP) for Ti samples in NaCl was measured at first. To acquire a stable value of OCP, the Ti sample was left alone in solution for around 30 minutes before measuring. The potential sweep was set in the range between OCP ± 0.5 V with a rate of 1 mV per second.

Electrochemical impedance spectroscopy (EIS) of Ti samples were examined by the same system (Versastat-3, Princeton Applied Research, USA) in 3.5wt% of NaCl solution at 37°C. The following parameters are set before measuring the EIS; initial potential (0 V), high frequency (10^6 Hz), low frequency (0.1 Hz), and amplitude (0.005 V). All data were processed by the installed software VersaSTAT 3.

Preprints.org (www.preprints.org) | NOT PEER-REVIEWED | Posted: 2 June 2023 doi:10.20944/preprints202306.0173.v1

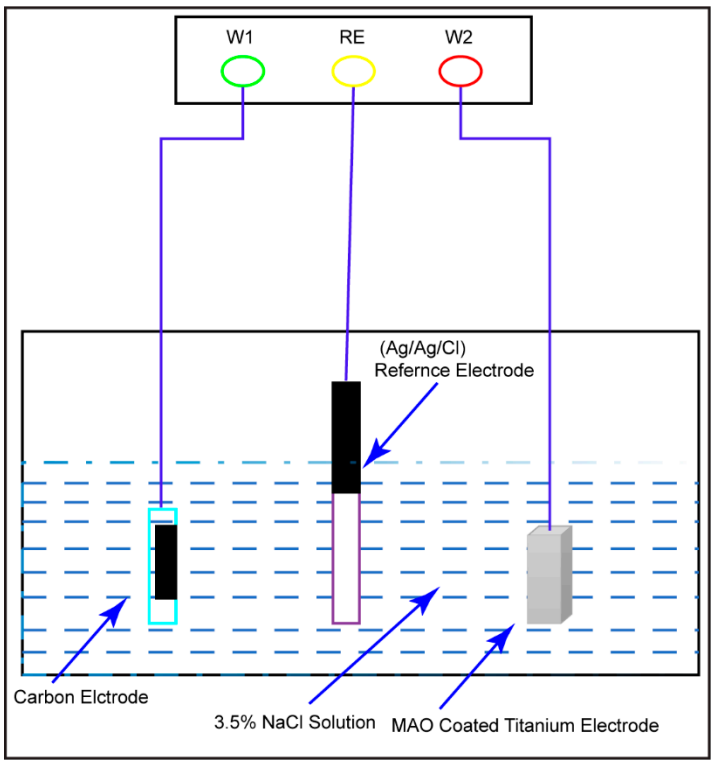

Figure 3. The schematics for potentiodynamic test of untreated, MAO and ECAP treated CP Ti.

2.3.1. Tafel extrapolation

The corrosion current density, i_{corr} (mA cm^{-2}), is computed using Tafel extrapolation of polarization curves, and the corrosion rate, Y_i (mm $year^{-1}$), can be determined using this value.

$$Y_i = 11.85 i_{corr} \quad (2)$$

Before utilizing the cathodic extrapolation method, it is suggested to measure both the anodic and cathodic branches of the polarization curve to obtain a more accurate estimate of the corrosion rate [54].

2.3.2. Electrochemical Impedance Spectroscopy

To calculate the corrosion current density, i_{corr} (mA cm^{-2}), we determine the polarization resistance, $R_p(\Omega\ cm^2)$, using electrochemical impedance spectroscopy (EIS).

$$i_{corr} = \frac{\beta_a \beta_c}{2.3 R_p (\beta_c - \beta_a)} = \frac{B}{R_p} \quad (3)$$

Where $B = \frac{\beta_a \beta_c}{2.3 (\beta_c - \beta_a)}$.

The corrosion rate, $Y_{i,EIS,}$ may be calculated using the formula in equation 2: Where β_a *and* β_c are the anodic and cathodic Tafel slopes, respectively. Values for β_a *and* β_c are calculated using an iR adjusted polarization curve [54,55].

2.4. Material Characterization

2.4.1. X-ray diffraction (XRD)

The microstructure of deposited films by MAO is examined by The X-ray diffractometer (XRD, PANalytical XPert PRO MPD) used monochromatic high intensity Cu Kα radiation (λ=1.5425 Å) was used to determine the crystal structures of deposited films. The mode is set to thin film and scanning angle was from 10°–2θ to 80°–2θ, with a step size of 0.03°, measuring time of 1.0 s per step and incident angle 0.5°.

The crystal size of films D can be calculated according to Scherrer's formula

 doi:10.20944/preprints202306.0173.v1

$$D = \frac{k\lambda}{\beta\cos\theta} \quad (4)$$

where k is the shape factor (0.9), λ the wavelength of X-rays (1.5425 Å), θ the scattering angle of the crystal plane and β the full width at half maximum (FWHM) of the peak. The analysis was numerically calculated by Jade® 5 (Materials. Data Inc., CA USA).

2.4.2. Elemental Composition (EDS)

The elemental compositions of deposited films were examined by energy-dispersive X-ray spectrometer (EDS, Bruker Nano, XFlash Dectector 6|10, Germany). The operating voltage and current were set to 15.0 kV and 55.0 μA respectively. Selection of target elements depends on the compositions of films. In this study, we focus on C, O, P, Ca and Ti to determine the main chemical compositions of deposited films by MAO. The scanning electron microscope (SEM) image size is 1024 × 768 pixels with magnification of 3000x for all samples and the averages of element compositions were calculated subsequently.

2.4.3. Surface Morphology

The morphology of deposited films by MAO is imaged by scanning electron microscope (SEM, S-3400N, Hitachi, Japan). For SEM imaging, the voltage of accelerated electron beam is set at 15 kV and the magnification is chosen to be 1,000 to 3,000 for the best resolution and overall view.

2.5. Biomedical Investigation

2.5.1. Pulp and Periodontal Cells on Modified Titanium

Pulp and periodontal cells were grown in trypsin for 1, 3, and 7 days. The enzyme-linked immunosorbent assay (ELISA) and AlamarBlue reagent were utilized to assess the viability of cells. For the experiment, commercially pure titanium specimens were produced through sterilization at 124 degrees Celsius. To create a culture medium, the extracted pulp and periodontal cells were digested with trypsin. Then, 24 petri dishes containing four of each species were prepared. After 15 to 45 minutes, pulp and periodontal cells settled and adhered to titanium surfaces where they were titrated. A mixture of 10% fetal bovine serum and DMEM, comprising 1 mL, was added to each well. The samples were kept in an incubator with temperature and humidity controls for 1, 3, and 7 days. After the required incubation periods, ten micrometers of AlamarBlue dye were added to each specimen, and 200 micrometers of the medium were removed and deposited in a new 96-well petri dish. Using the ELISA method, the responses of pulp and periodontal cells to the extracted media were assessed. This study clarified their ability to persist on titanium surfaces that had been modified.

3. Results and Discussion

3.1. Sever Plastic Deformation

In this investigation, molybdenum disulfide (MoS_2) was used because of its proven record of success in decreasing friction and wear between the billet material and the die under extreme plastic deformation at temperatures as high as 400 degrees Celsius. The states of the CP-Ti samples are shown in the **Figure 4A** below, from their "as-received" state to after both one and two passes of ECAP. After every plunge, the billet was rotated counterclockwise by 90 degrees to reverse the direction of the applied plunger force. Evidenced by the presence of black spots on each sample after one and two passes, which correspond to the MoS2 lubricant, the ECAP deformation figures show the significant deformation of the CP-Ti samples in both passes. More importantly for future mechanical and biological characterizations, the findings show that homogenous deformation was achieved in the CP-Ti samples. **Figure 5B** demonstrates that the total equivalent plastic deformation increases as the number of passes increases, as predicted by Equation 1. For future trials using titanium, the number of passes must be increased. This investigation is limited to a maximum of two

 doi:10.20944/preprints202306.0173.v1

passages, as it has been demonstrated that this is sufficient for enhancing the mechanical properties of Cp Ti.

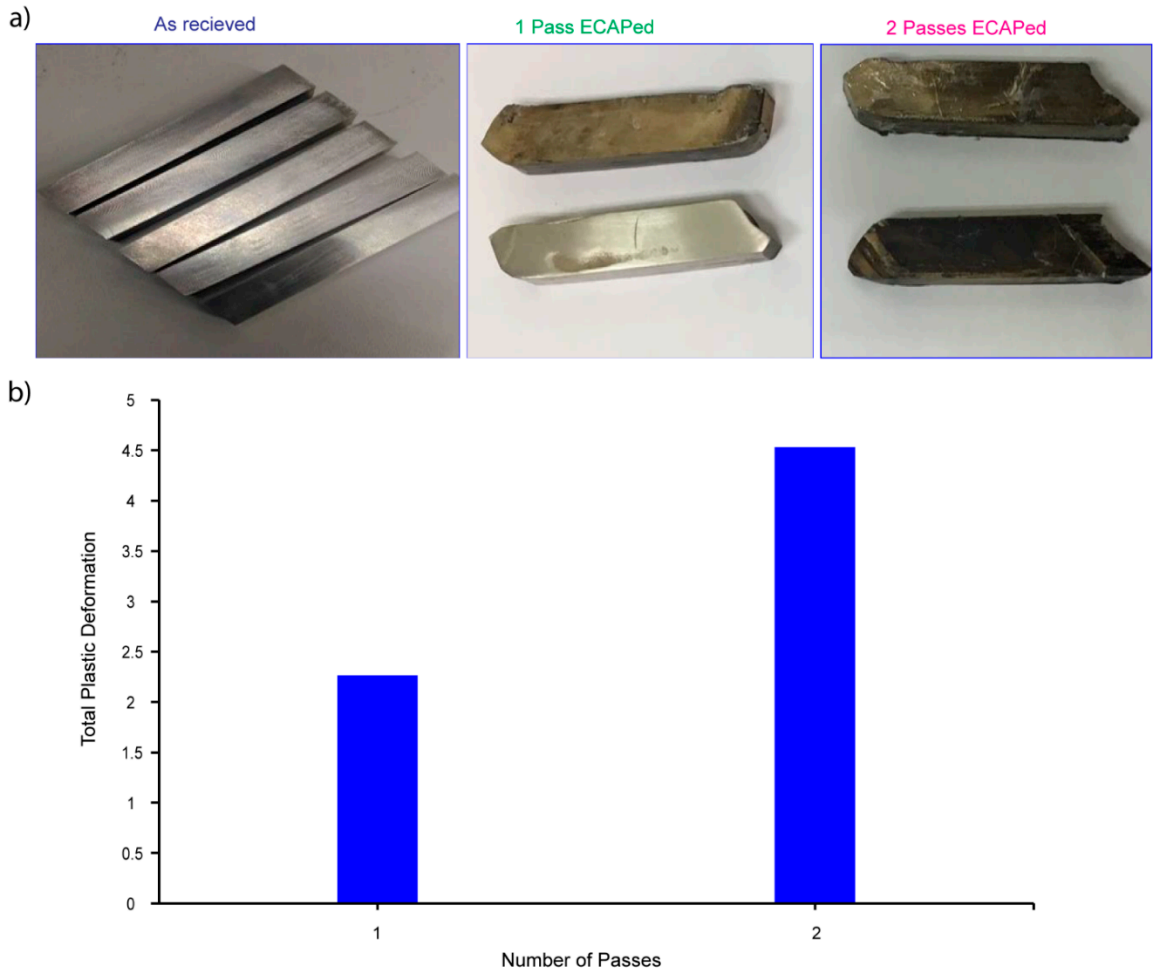

Figure 4. A) CP Ti as received, 1 pass, 2 pass ECAP treated at 400^{0}C using MoS_2 lubrication and B)Total plastic deformation with number of passes.

3.2. X-ray diffraction

When combined, ECAP and MAO can enhance the mechanical and surface properties of CP Ti for medical applications. After being in contact with CP Ti that had been treated with ECAP and MAO, human dental pulp cells and periodontal cells proliferated and differentiated better. The X-ray diffraction pattern is shown in **Figure 5** for 0-, 1- and 2-pass Ti samples where crystal planes were numerically fitted by Gaussian curves and identified using the database in Jade® 5. According to the fitting results, only crystalline phases of Ti can be firmly identified. Peaks of anatase TiO_2 from the database in Jade® are all marginally shifted by several tenth degrees away from the Gaussian fittings. This shift could be attributed the small sizes of TiO_2 crystallites. In other words, the anatase phases are somewhat amorphous or minute produced by the micro-arcing process. It is interesting to notice that none of the crystal structures of phosphor, calcium or carbon were found in the XRD pattern. To further examine the deposited film, the following EDS provides us extra information about the elemental compositions inside the film.

The X-ray diffraction (XRD) pattern is a powerful tool for identifying the crystal structure and phase composition of materials. In the study presented, the XRD pattern was used to analyze the crystal structure of Ti samples subjected to different passes. The fitting results of the Gaussian curves showed that only the crystalline phases of Ti could be identified. This finding is in line with previous studies that have shown that Ti has a predominantly crystalline structure [56].

 doi:10.20944/preprints202306.0173.v1

Interestingly, the anatase phase of TiO_2 was found to be marginally shifted by several tenth degrees away from the Gaussian fittings. This shift could be attributed to the small size of TiO_2 crystallites, which renders the anatase phases somewhat amorphous or minute, as produced by the micro-arcing process. This observation is consistent with previous studies that have reported similar shifts in the XRD pattern of TiO_2 due to the reduction in the size of crystallites [57].

Another notable finding of this study is that none of the crystal structures of phosphor, calcium, or carbon were found in the XRD pattern. This suggests that the deposited film mainly consists of Ti with some minor impurities. The absence of these impurities is consistent with previous studies that have shown that micro-arc oxidation (MAO) Ti coatings have high purity due to the unique process used to produce them [58].To further examine the deposited film, the study used energy-dispersive X-ray spectroscopy (EDS) to obtain elemental compositions. The results showed that the film contained only Ti and oxygen, with a negligible amount of impurities. This finding is consistent with previous studies that have reported the high purity of TiO_2 coatings produced by MAO [59].In conclusion, the XRD pattern and EDS analysis provided valuable insights into the crystal structure and elemental composition of Ti samples produced by micro-arc oxidation. The findings of this study are consistent with previous studies and add to our understanding of the properties of TiO_2 coatings produced by MAO.

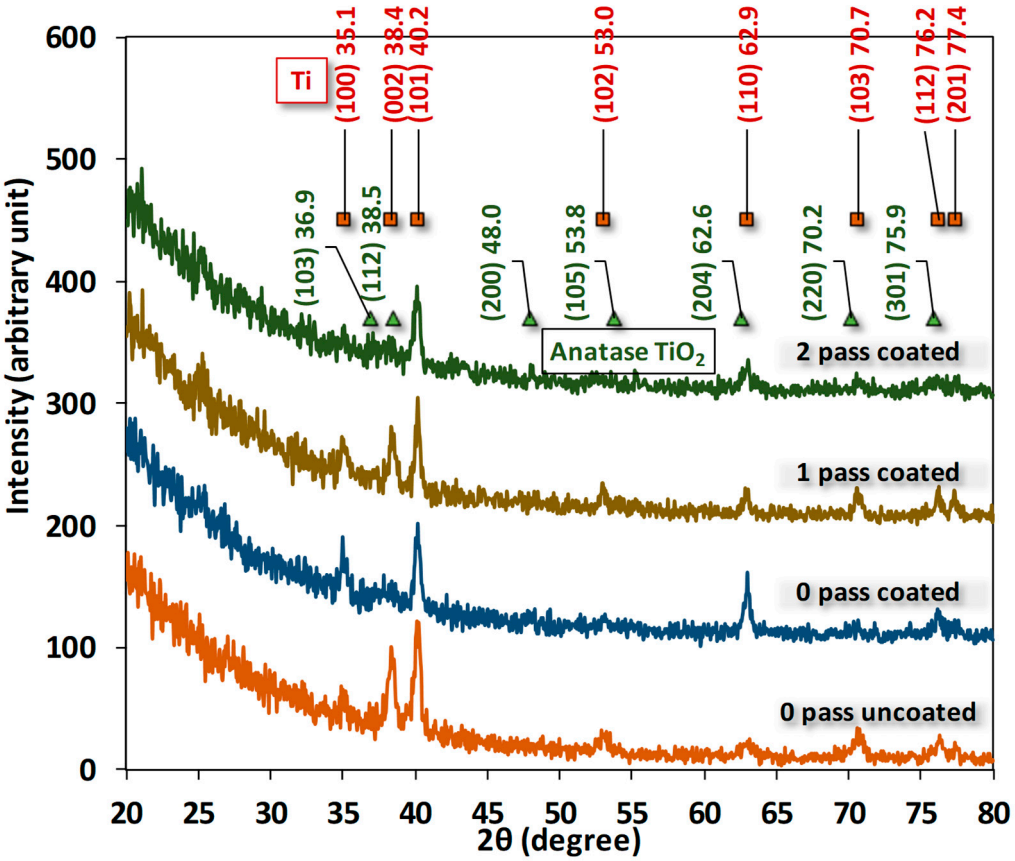

Figure 5. The XRD Image of grade 4 Ti before and after ECAP treatments and micro-arc oxidation for coating.

3.3. SEM and EDS

The mapping of chemical elements on the surface of deposited films by micro-arcing are shown in **Figure 6** where the image is taken for 0-, 1- and 2-pass Ti substrate by magnification of 3000. The deposited films are multiple layers and obviously porous. The pore size and density are quite the same, which means the ECAP processed Ti substrate has little influence on the deposited films by micro-arc.

 doi:10.20944/preprints202306.0173.v1

Several other studies have investigated the microstructure and properties of TiO_2 coatings produced by MAO. The coatings exhibited a mixed-phase structure of anatase and rutile, which is not consistent with the findings of this study [60]. One investigation [61] demonstrated that the TiO_2 coatings produced by MAO exhibited better corrosion resistance than bare Ti substrates, while other study [56] found that the coatings exhibited good mechanical properties and wear resistance. Research result [58] showed that the TiO_2 coatings produced by MAO could potentially be used as protective coatings for titanium alloys, and a study [45] found that the coatings exhibited good biocompatibility, making them suitable for use as implant coatings. Finally, another study [61] demonstrated that the TiO_2 coatings produced by MAO exhibited good corrosion resistance and wear resistance, further supporting the potential use of such coatings in various applications.

Taken together, these studies demonstrate the versatility and potential of TiO_2 coatings produced by MAO in various fields, including corrosion resistance, mechanical strength, wear resistance, and biocompatibility. The findings of this study contribute to the growing body of research on the properties and potential applications of MAO Ti coatings, highlighting the need for further investigation and development of such coatings in various fields.

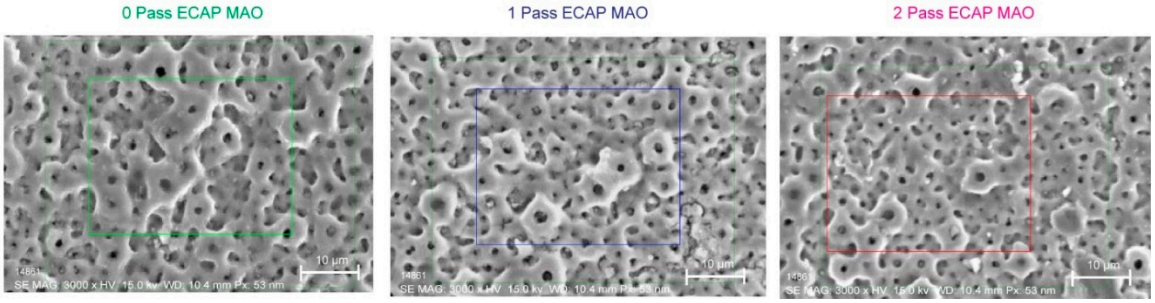

Figure 6. The SEM result of grade 4 CP Ti after ECAP treatment and micro-arc oxidation for coating.

To further identify the composition of films, we examined the elemental mapping in the area of these SEM images. **Figure 7** shows the mapping results for each Ti substrate and three important elements, namely, phosphorus, calcium, and carbon, are clearly found. In other words, the deposition by micro-arc is successfully to deliver these elements from the aqueous electrolytes: calcium glycerophosphate hydrate ($C_7H_7CaO_6P$-$2H_2O$) and calcium acetate ($Ca(CH_3COO)$-$2H_2O$). The EDS mapping is conducted for all three passes with Micro arc oxidation coating applied namely, 1 pass, 2 pass, and 3 pass of titanium specimen.

However, since XRD does not present any crystalline phase containing or related to these elements, that means these films are most likely to be amorphous.

The results of a study that applied both techniques to titanium specimens have been presented in this paper, and the elemental mapping and XRD analysis of the coated specimens were discussed.

The elemental mapping results presented in **Figure 7** clearly show the successful deposition of three important elements, namely, phosphorus, calcium, and carbon, onto the titanium substrate using the micro arc oxidation technique. This observation is consistent with previous studies that have reported the ability of MAO to deliver various elements onto the surface of metals through the electrolyte solution used during the process [62]. The presence of these elements on the surface of the titanium substrate is expected to improve its biological properties, such as osseointegration, which is important for biomedical applications [26].

It is worth noting that the absence of any crystalline phase containing or related to these elements in the XRD analysis suggests that the films are most likely amorphous. This observation is consistent with previous studies that have reported the formation of amorphous films on titanium substrates using the MAO technique [63–65]. The amorphous nature of the films can have both advantages and disadvantages. For example, amorphous films can have improved mechanical properties, such as hardness, compared to crystalline films [66,67]. On the other hand, the stability and long-term behavior of amorphous films are not well understood, and they can be prone to degradation over time [68].

 doi:10.20944/preprints202306.0173.v1

In summary, the results of this study indicate the successful deposition of important elements onto the surface of titanium substrates using the micro arc oxidation technique. The films were found to be amorphous, which can have both advantages and disadvantages depending on the application. Further studies are needed to fully understand the long-term behavior and stability of these films.

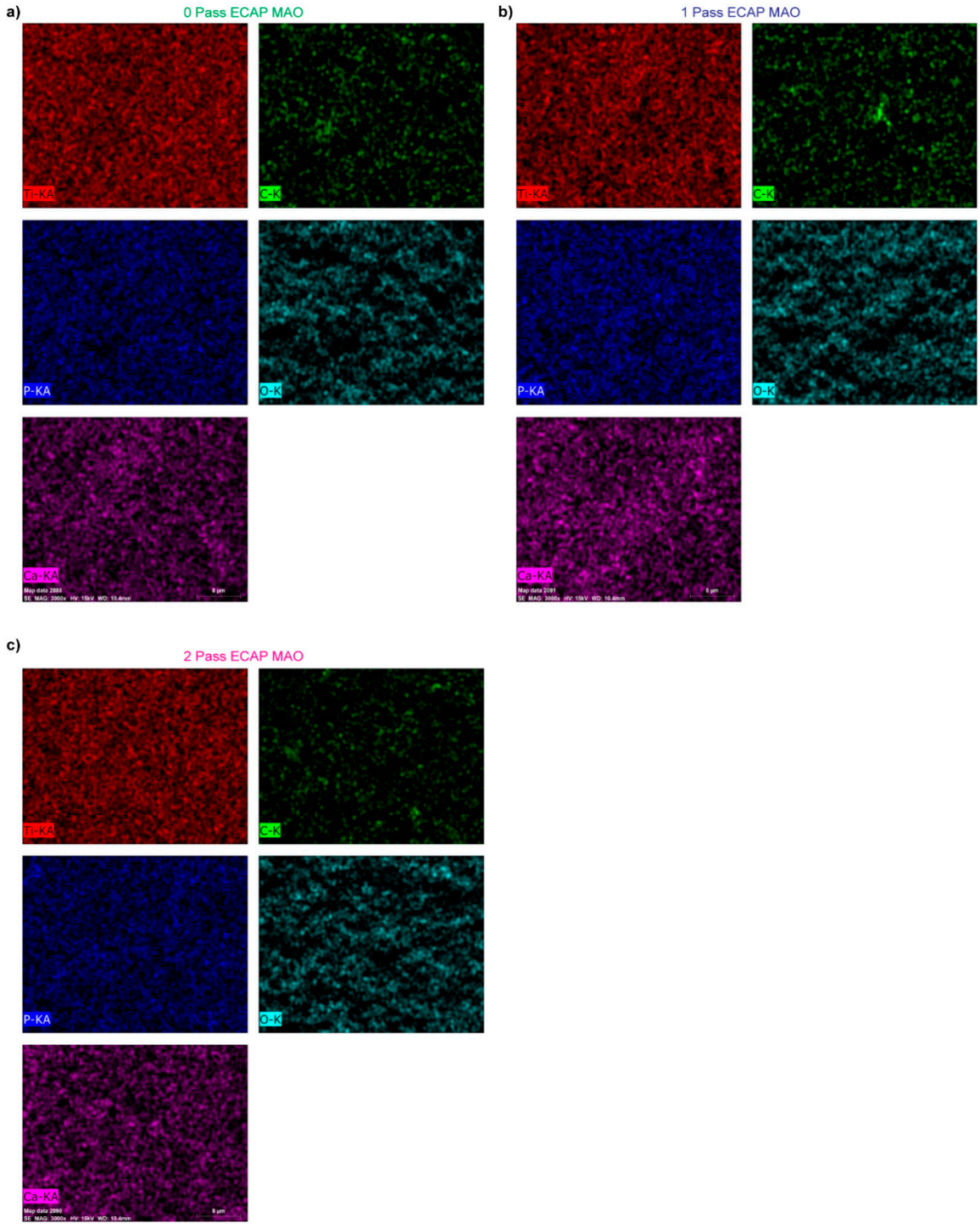

Figure 7. The elemental mapping from the area shown in the SEM image of A) as received, B) one pass ECAP, and C) 2 pass ECAP grade 4 Ti after micro-arc oxidation for coating.

The quantitative of element compositions in these mapping areas are presented in **Figure 8A** for the average weight percentage of each mapped element. The major elements in the area, as expected, are Ti and O. Both account for slightly more than 80%. The rest are carbon, phosphorus, and calcium.

 doi:10.20944/preprints202306.0173.v1

Among these three, calcium is more than the other two because the two electrolytes in micro-arc all have calcium as their main constituent.

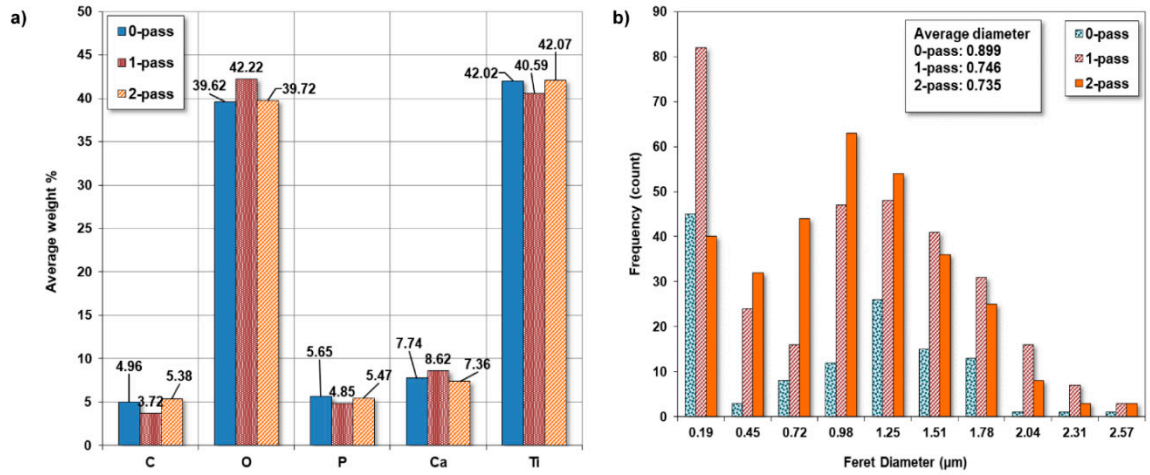

Figure 8. A) The average weight percentage of elements from EDS mapping and B) the Pore size of the coating on the samples.

3.3.1. Pore Size.

Utilizing ImageJ software to analyze the microstructure SEM image, a graph was generated to depict the frequency of ferret diameter for commercially pure titanium with 0-pass, 1-pass, and 2-pass. The obtained results indicated that the average diameter was 0.899, 0.746, and 0.735 micrometers, respectively as shown in **Figure 8B**.

The main objective of this study was to investigate the influence of pass number on the microstructure of commercially pure titanium. The findings of this study revealed a decline in the average ferret diameter as the pass number increased. This result is in line with the previous research which reported a decrease in grain size with an increase in the pass number during the cold rolling process of titanium [69].

However, in contrast to the study which reported an increase in grain size with an increase in the pass number, the present study exhibited contradictory results. This could be attributed to the differences in processing techniques or the purity of the titanium used in the study [70]. Furthermore, the microstructure of the 2-pass sample revealed a more refined structure than the 0-pass sample. This observation is consistent with the research which indicated that multi-pass rolling leads to a refined microstructure and improved mechanical properties of titanium [71].

3.4. Tafel Plot

Figure 9 represents the results of a potentiodynamic Tafel plot analysis conducted on commercially pure titanium samples with varying degrees of coating and passes. The Tafel plot technique is used to study the corrosion behavior of metallic materials by plotting the logarithm of the corrosion current density against the electrode potential. The potential values in the table represent the electrode potential values measured during the analysis.

The plot is made by measuring the anodic and cathodic currents on a logarithmic scale as a function of the applied potential. The slope of the Tafel line gives information on the kinetics of electrochemical reactions, and the intersection of the anodic and cathodic Tafel lines gives information about corrosion characteristics. The formula below can be used to determine the corrosion parameters from the Tafel Plot.

From the results presented in **Figure 9**, it can be observed that the electrode potentials for the uncoated samples are relatively lower than those of the coated samples. The uncoated samples show a gradual increase in electrode potential as the number of passes increases, from 1.12 V for 0-pass to 1.15 V for 1-pass and 1.18 V for 2-pass, indicating a gradual decrease in the corrosion rate as the

 doi:10.20944/preprints202306.0173.v1

number of passes increases. This trend is expected because the more the metallic surface is covered, the less susceptible it is to corrosion.

On the other hand, the coated samples show a significant increase in electrode potential values compared to the uncoated samples. The 0-pass coated sample has an electrode potential of 1.44 V, which is significantly higher than that of the uncoated 0-pass sample (1.12 V). The electrode potentials for the 1-pass and 2-pass coated samples are the same (1.48 V), indicating that further coating does not provide additional protection against corrosion. This suggests that the coating is highly effective in reducing the corrosion rate of the metallic sample.

The results of the Tafel plot analysis suggest that the coating significantly reduces the rate of corrosion compared to the uncoated samples. The increase in electrode potential values of the coated samples indicates that the coating provides a more stable and passive layer, preventing the metallic samples from further corrosion. The effect of additional coating passes appears to be limited, with no significant change in electrode potential observed between 1-pass and 2-pass coated samples. Overall, the results suggest that the coating significantly enhances the corrosion resistance of the metallic samples. The findings could be useful in designing and developing more effective corrosion-resistant coatings for industrial applications.

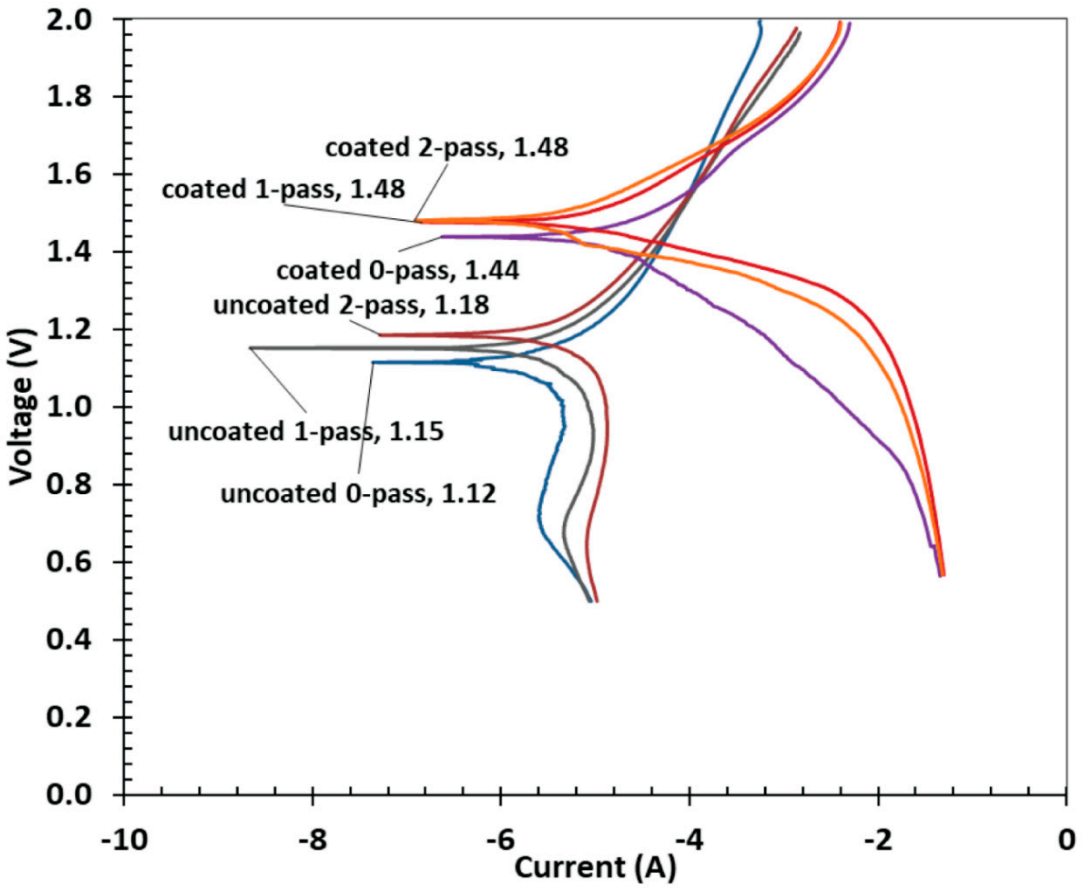

Figure 9. The Tafel plot for open circuit voltage for SEM of grade 4 Ti before/after micro-arc oxidation for coating.

3.4.1. Corrosion Loss

The data presented in **Table 1** provides a view on the effectiveness of coatings in reducing the corrosion rate of commercially pure titanium samples. This finding is consistent with previous research studies that have examined the impact of coatings on metallic materials. This experiment conducted a similar study on a titanium alloy and discovered that the corrosion resistance of the alloy significantly increased with the use of a protective coating [72].

Preprints.org (www.preprints.org) | NOT PEER-REVIEWED | Posted: 2 June 2023 doi:10.20944/preprints202306.0173.v1

Table 1. corrosion behavior parameters calculated from the Tafel plot.

Samples	E_{corr} (V)	B_a (V)	B_c (V)	R_p (Ohms.cm^2)	i_{corr} (μA/cm^2)	CR mpy
CG	1.21	0.01	2.18	0.01	0.70	0.97
UFG1	1.49	0.04	0.07	0.08	0.59	0.81
UFG2	1.16	0.00	0.25	0.00	0.53	0.72
CGMAO	1.52	0.04	0.11	0.05	0.51	0.71
UFG1AMO	1.11	0.02	0.31	0.02	0.51	0.70
UFG2MAO	1.47	0.20	0.16	-0.83	0.48	0.66

Ecorr : Corrosion Potential; I_{corr} : Corrosion current; B_a : Anodic Slope; B_c : Cathodic Slope CG : uncoated 0-pass ECAP ; UFG1 : uncoated 1-pass ECAP; UFG2 : uncoated 2-pass ECAP; CGMAO : coated 0-pass; UFG1MAO : coated 1-pass ECAP; UFG2MAO : coated 2-pass ECAP

In their study, the coating's thickness and composition had a significant effect on the metal corrosion resistance. However, the effectiveness of the coating in reducing the corrosion rate of the metal depends on the selection of the coating material and method of application. Discovering the most effective coatings for various metallic materials and applications requires additional research.

The corrosion loss, expressed in miles per year (mpy), was used in equation 1 to calculate the corrosion resistance of the samples. The samples were labeled as follows: CG (untreated), UFG1 (after one ECAP pass), UFG2 (after two ECAP passes), CGMAO (after MAO treatment), UFG1MAO (after 1 pass ECAP treatment followed by MAO treatment), and UFG2MAO (after 2 pass ECAP treatment followed by MAO treatment).

According to the corrosion loss measurement data in **Table 1 and Figure 10D**, UFG2MAO had the lowest corrosion rate (0.65 mpy), followed by UFG1MAO (0.70 mpy), CGMAO (0.71 mpy), UFG2 (0.72 mpy), UFG1 (0.81 mpy), and CG (0.97 mpy). These findings indicate that increasing titanium's corrosion resistance can be accomplished by combining SPD, ECAP, and MAO surface modification.

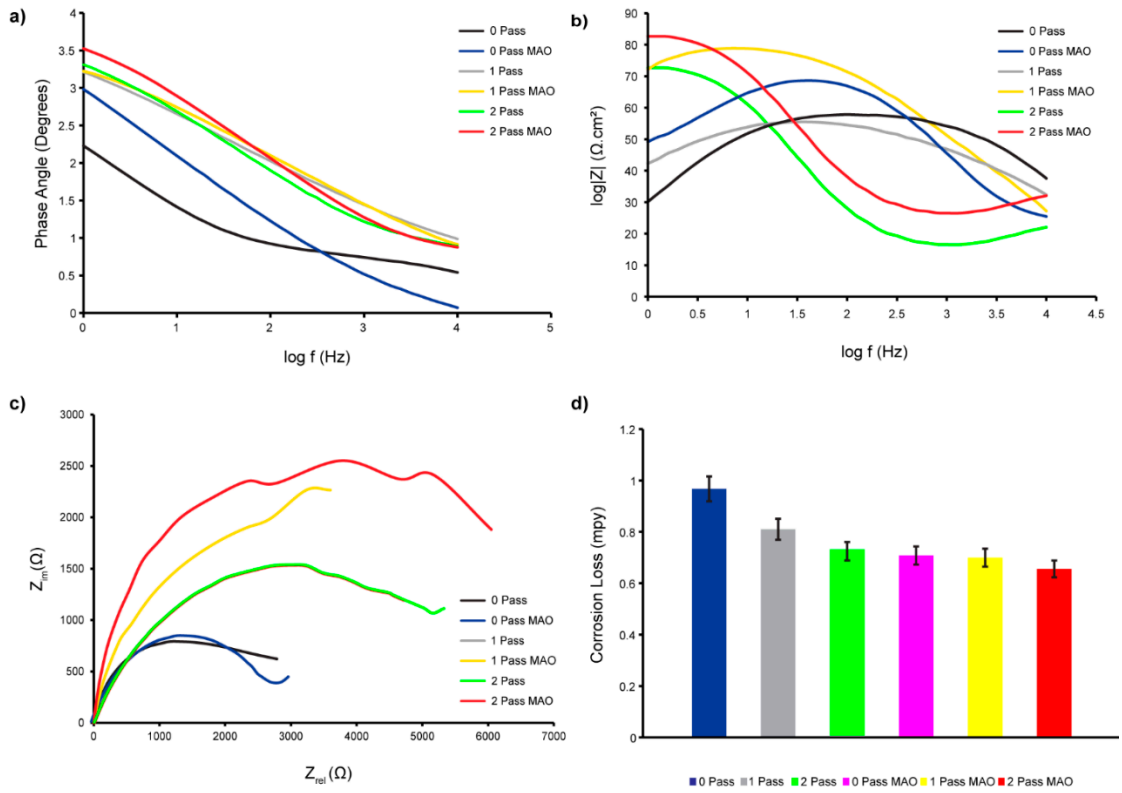

Figure 10. shows the corrosion loss in miles per year of ECAP and MAO treated samples.

 doi:10.20944/preprints202306.0173.v1

Numerous studies have examined the effect of ECAP and MAO surface modification on the corrosion resistance of Ti and its alloys. For example, after ECAP treatment, the grain size of pure Ti was refined and the density of dislocations was increased, resulting in substantially improved corrosion resistance [73]. Additionally, ECAP treatment and subsequent MAO surface modification improved the corrosion resistance of Ti-6Al-4V alloy [72,73].

Figure 10A demonstrates that the phase angle of the sample treated with 2-pass ECAP and MAO is greater at lower frequencies. A larger phase angle indicates that the system exhibits greater capacitance. This type of behavior has been linked to the formation of a barrier layer on the surface of the substrate, in this instance the 2-pass ECAP and MAO-treated sample. By preventing the passage of charge, this protective coating significantly slows down the corrosion process. Thus, a larger phase angle at low frequencies is frequently indicative of a more effective and protective coating. Unlike the UFGMAO sample, due to its higher frequency and lower phase angle, the CGMAO sample is more susceptible to corrosion. **Figure 110B** depicts the Bode graphs; the absolute value of Z in UFGMAO titanium is greater at lower frequencies. Interpreting this behavior, a greater absolute value of Z at lower logarithmic frequencies indicates increased impedance or corrosion resistance. This suggests that the formation of a protective oxidation layer on the surface of the material is responsible for the increased corrosion resistance observed at lower frequencies in titanium treated with 2 passes of ECAP and MAO. This oxide layer acts as a barrier, reducing corrosion by isolating the metal from its corrosive environment.

The Nyquist Plot depicted in **Figure 10C** enables us to conclude that the UFGMAO sample has the highest value of Z imaginary in ohms. Compared to the other samples, this indicates a reduced corrosion rate. It also indicates that MAO and multi-pass ECAP have the potential to enhance CP Ti's corrosion resistance. **Figure 10C** indicates that the CG sample is more corroded than the other samples, indicating a higher corrosion rate.

It has been hypothesized that MAO surface modification increases the corrosion resistance of Ti and its alloys via the formation of a protective oxide layer on the surface of the material. The MAO treatment generates surface fissures containing Ca-P minerals that promote the formation of bioactive hydroxyapatite [74]. The hydroxyapatite layer provides a stable and protective contact between the material and the corrosive environment by acting as a barrier to prevent the diffusion of corrosive ions.

3.5. Biomedical Experiment

At the National Taiwan University Hospital, researchers studied cell proliferation in four distinct sample materials in an in vitro investigation. Pulp cells and human periodontal ligament cells both showed different levels of mitochondrial activity. Significantly greater absorbance values were seen on day 3 for cells grown on CG and CG with MAO surfaces compared to cells grown on UFG and UFG with MAO surfaces on day 1, as shown in **Figure 11A**. Furthermore, on day 7, there were substantial variations in absorbance across CG and UFG surfaces. Despite seeming to contradict several other studies [75], these results nonetheless provide novel scientific insights.

As depicted in **Figure 11B** Another significant result involved human periodontal ligament cells, where the number of cells on UFG-MAO was significantly higher than on UFG after 1 and 7 days, with similar numbers observed after 3 days. Human pulp cells underwent a three-day viability test with four titanium samples (CG, CGMAO, UFG, and UFGMAO) and a TCPS control group. On each of the three sampling days, the CG and UFG samples had lower pulp cell viability than the TCPS control group as shown in **Figure 11A**. On day 3, there was no difference in pulp cell viability between CGMAO and UFGMAO samples and CG and UFG. Using micro arc oxidation (MAO) technology and mineral solutions containing Ca and P to modify commercially pure titanium samples (CGMAO and UFGMAO) may improve pulp cell viability; however, additional research is necessary to optimize processing procedures and improve biocompatibility for medical implants. This study may appear to contradict other research, but it contributes to the corpus of scientific knowledge on the subject.

Preprints.org (www.preprints.org) | NOT PEER-REVIEWED | Posted: 2 June 2023 doi:10.20944/preprints202306.0173.v1

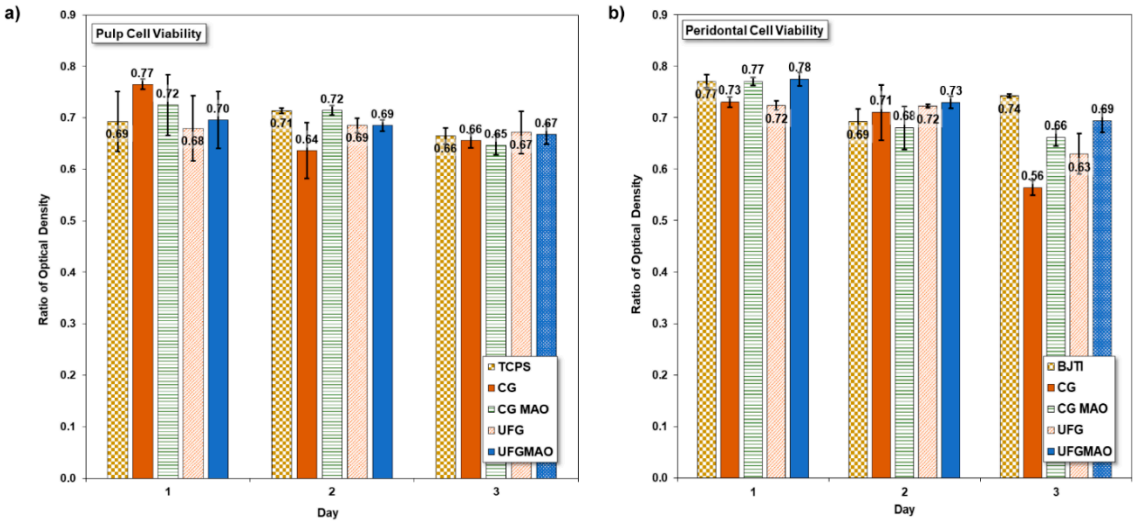

Figure 11. The viability test for a) human pulp cells using the control group TCPS and b) human periodontal cells utilized the control group BJTI on different titanium samples (CG, CGMAO, UFG, UFGMAO).

The success or failure of medical implants depends on their biocompatibility, or their ability to integrate with the body. Micro arc oxidation (MAO) technology was used to modify commercially pure titanium (CG and UFG) with mineral solutions containing Ca and P (CGMAO and UFGMAO), and then the materials' ability to support the viability of periodontal cells was evaluated. The periodontal cell viability of all titanium samples and the BJTI control sample decreased over time, with the CG and UFG samples consistently demonstrating lower vitality than the BJTI control sample over the course of three days. On days 3 and 7, the periodontal cell viability of the CGMAO and UFGMAO samples were lower than that of the BJTI control group as depicted in **Figure 11B**. In terms of periodontal cell survival, the CGMAO and UFGMAO samples outperformed the unmodified CG and UFG samples on day 1, but by days 3 and 7, the difference had dissipated. On day 7, the periodontal cell viability of the CGMAO and UFGMAO samples were greater than that of the CG and UFG samples, but lower than that of the BJTI control group.

Our findings indicate that periodontal cell viability can be enhanced on samples of commercially pure titanium by modifying the surface with MAO technology and mineral solutions, including Ca and P. Further research is required to optimize titanium refining procedures for greater biocompatibility in medical implants, as periodontal cell survival on all titanium samples remained inferior to that of the BJTI control group. Our research provides information regarding the biocompatibility of titanium samples intended for use in medical implants. Using cutting-edge MAO and SPD technologies to maximize periodontal cell survival on titanium substrates. Titanium implants have the potential to improve patient outcomes if these techniques can be optimized through further research.

4. Conclusion

Micro arc oxidation (MAO) technology, mineral solutions containing Ca and P, and the equal channel angular pressing (ECAP) method for severe plastic deformation (SPD) can be used to improve the mechanical properties of CP Ti and its cell viability, which were observed through this study. The following findings of this study could be draw:

- The surface modification process using MAO and mineral solutions containing Ca and P can change the composition and shape of the surface of pure titanium.
- The corrosion resistance of commercially pure titanium can be enhanced by integrating ECAP and MAO surface modification.
- Human pulp and periodontal cell viability can be enhanced by modifying commercially pure titanium samples (CGMAO and UFGMAO) with micro arc oxidation (MAO) and ECAP

 doi:10.20944/preprints202306.0173.v1

technology; however, additional testing methods must be developed for improved biocompatibility in medical implants.

Overall, the results indicate that ECAP and MAO may be combined to enhance the mechanical properties of purified titanium, which is beneficial for biomedical applications. Future biomedical engineering research may benefit from the findings because they provide understanding on the behavior of dental pulp cells and periodontal cells. Therefore, the findings of this study will contribute to the development of cutting-edge biomedical implants with enhanced functionality for extended durations.

Author Contributions: Conceptualization, D.B.A and S.J-H.; methodology, D.B.A, S.J-H C.L. and J.H.H.; software, D.B.A, M.T, J.H.H. and S.J-H.; validation, D.B.A,S.J-H. and M.T.; formal analysis, D.B.A.; investigation, D.B.A.; data curation, D.B.A,; writing—original draft preparation, D.B.A and C.L; writing—review and editing, D.B.A., M.T., C.L. and S.J-H.; supervision, M.T. and S.J.H; project administration, S.J-H and M.T. All authors have read and agreed to the published version of the manuscript.

Funding: This research was funded by the MINISTRY OF SCIENCE AND TECHNOLOGY OF TAIWAN (project No. MOST-105-2221-E-011-058-MY2).

Data Availability Statement: Not applicable.

Acknowledgments: The authors would like to acknowledge the financial support from the Ministry of Science and Technology of Taiwan (project No. MOST-105-2221-E-011-058-MY2).

Conflicts of Interest: The authors declare no conflict of interest.

References

1. Agarwal, K.M., Tyagi, R.K., Singhal, A., Bhatia, D.: Effect of ECAP on the mechanical properties of titanium and its alloys for biomedical applications. Mater. Sci. Energy Technol. 3, 921–927 (2020). https://doi.org/10.1016/j.mset.2020.11.002
2. Niinomi, M.: Mechanical biocompatibilities of titanium alloys for biomedical applications. J. Mech. Behav. Biomed. Mater. 1, 30–42 (2008)
3. Elias, C.N., Lima, J.H.C., Valiev, R., Meyers, M.A.: Biomedical applications of titanium and its alloys. Jom. 60, 46–49 (2008)
4. Arora, H.: Titanium: The Ideal Dental Implant Material Choice BT - Surface Modification of Titanium Dental Implants. Presented at the (2023)
5. Bordbar-Khiabani, A., Gasik, M.: Electrochemical and biological characterization of Ti–Nb–Zr–Si alloy for orthopedic applications. Sci. Rep. 13, 2312 (2023). https://doi.org/10.1038/s41598-023-29553-5
6. Hussein, M.A., Azeem, M.A., Kumar, A.M., Saravanan, S., Ankah, N., Sorour, A.A.: Design and processing of near-β Ti–Nb–Ag alloy with low elastic modulus and enhanced corrosion resistance for orthopedic implants. J. Mater. Res. Technol. 24, 259–273 (2023). https://doi.org/https://doi.org/10.1016/j.jmrt.2023.03.003
7. Aslan Çakır, M., Yetim, T., Yetim, A.F., Çelik, A.: Superamphiphobic TiO2 Film by Sol–Gel Dip Coating Method on Commercial Pure Titanium. J. Mater. Eng. Perform. (2023). https://doi.org/10.1007/s11665-023-08049-3
8. Pesode, P., Barve, S., Wankhede, S. V, Jadhav, D.R., Pawar, S.K.: Titanium alloy selection for biomedical application using weighted sum model methodology. Mater. Today Proc. 72, 724–728 (2023). https://doi.org/https://doi.org/10.1016/j.matpr.2022.08.494
9. Aslantas, K., Demir, B., Guldibi, A.S., Niinomi, M., Dikici, B.: A comparative study on the machinability of β-type novel Ti29Nb13Ta4.6Zr (TNTZ) biomedical alloys under micro-milling operation. J. Manuf. Process. 92, 135–146 (2023). https://doi.org/https://doi.org/10.1016/j.jmapro.2023.02.043
10. Barboza, K., Carobolante, A., Rajan, S.S., Bortolini, C., Sabino, R.M., Nakazato, R.Z., Popat, K.C., Paula, A., Alves, R.: Studies of the New Ti-25Ta-25Nb-5Sn Alloy. 1–13 (2023)
11. Shi, X., Wang, X., Chen, B., Umeda, J., Bahador, A., Kondoh, K., Shen, J.: Precision control of oxygen content in CP-Ti for ultra-high strength through titanium oxide decomposition: An in-situ study. Mater. Des. 227, 111797 (2023). https://doi.org/https://doi.org/10.1016/j.matdes.2023.111797
12. Elshalakany, A.B., Abdel-Mottaleb, M.M., Salunkhe, S., Alqahtani, B.: 7 - Mechanical properties of titanium

 doi:10.20944/preprints202306.0173.v1

alloys additive manufacturing for biomedical applications. In: Salunkhe, S., Amancio-Filho, S.T., and Davim, J.P.B.T.-A. in M.A.M. (eds.) Woodhead Publishing Reviews: Mechanical Engineering Series. pp. 219–231. Woodhead Publishing (2023)

13. Kati, J., Kriva˘, S.: Titanium Implant Alloy Modified by Electrochemically Deposited Functional Bioactive Calcium Phosphate Coatings. (2023)
14. Bandyopadhyay, A., Ciliveri, S., Bose, S.: Metal additive manufacturing for load-bearing implants. J. Indian Inst. Sci. 102, 561–584 (2022)
15. Soro, N., Brodie, E.G., Abdal-hay, A., Alali, A.Q., Kent, D., Dargusch, M.S.: Additive manufacturing of biomimetic Titanium-Tantalum lattices for biomedical implant applications. Mater. Des. 218, 110688 (2022)
16. Zhang, L., Chen, L.: A review on biomedical titanium alloys: recent progress and prospect. Adv. Eng. Mater. 21, 1801215 (2019)
17. Fernandes, D.J., Elias, C.N., Valiev, R.Z.: Properties and performance of ultrafine grained titanium for biomedical applications. Mater. Res. 18, 1163–1175 (2015)
18. Rack, H.J., Qazi, J.I.: Titanium alloys for biomedical applications. Mater. Sci. Eng. C. 26, 1269–1277 (2006)
19. Elias, C.N., Meyers, M.A., Valiev, R.Z., Monteiro, S.N.: Ultrafine grained titanium for biomedical applications: An overview of performance. J. Mater. Res. Technol. 2, 340–350 (2013)
20. Quinn, J., McFadden, R., Chan, C.-W., Carson, L.: Titanium for orthopedic applications: an overview of surface modification to improve biocompatibility and prevent bacterial biofilm formation. IScience. 23, 101745 (2020)
21. Mahajan, A., Sidhu, S.S.: Surface modification of metallic biomaterials for enhanced functionality: a review. Mater. Technol. 33, 93–105 (2018)
22. Asri, R.I.M., Harun, W.S.W., Samykano, M., Lah, N.A.C., Ghani, S.A.C., Tarlochan, F., Raza, M.R.: Corrosion and surface modification on biocompatible metals: A review. Mater. Sci. Eng. C. 77, 1261–1274 (2017)
23. Liu, L., Ma, F., Kang, B., Liu, P., Qi, S., Li, W., Zhang, K., Chen, X.: Preparation and mechanical and biological performance of the Sr-containing microarc oxidation layer on titanium implants. Surf. Coatings Technol. 129530 (2023)
24. Kumar, R., Agrawal, A.: Micro-hydroxyapatite reinforced Ti-based composite with tailored characteristics to minimize stress-shielding impact in bio-implant applications. J. Mech. Behav. Biomed. Mater. 105852 (2023)
25. Spriano, S., Yamaguchi, S., Baino, F., Ferraris, S.: A critical review of multifunctional titanium surfaces: New frontiers for improving osseointegration and host response, avoiding bacteria contamination. Acta Biomater. 79, 1–22 (2018)
26. Mitra, I., Bose, S., Dernell, W.S., Dasgupta, N., Eckstrand, C., Herrick, J., Yaszemski, M.J., Goodman, S.B., Bandyopadhyay, A.: 3D Printing in alloy design to improve biocompatibility in metallic implants. Mater. Today. 45, 20–34 (2021)
27. Modina, I.M., Dyakonov, G.S., Stotskiy, A.G., Yakovleva, T. V, Semenova, I.P.: Effect of the Texture of the Ultrafine-Grained Ti-6Al-4V Titanium Alloy on Impact Toughness. Materials (Basel). 16, 1318 (2023)
28. Nafikov, R.K., Kulyasova, O.B., Khudododova, G.D., Enikeev, N.A.: Microstructural Assessment, Mechanical and Corrosion Properties of a Mg-Sr Alloy Processed by Combined Severe Plastic Deformation. Materials (Basel). 16, 2279 (2023)
29. Sadrkhah, M., Faraji, G., Khorasani, S., Mesbah, M.: Excellent Mechanical Properties, Wettability and Biological Response of Ultrafine-Grained Pure Ti Dental Implant Surface Modified by SLActive. J. Mater. Eng. Perform. 1–14 (2023)
30. Huang, S., Ali, A.N.: Experimental investigations of e ff ects of SiC contents and severe plastic deformation on the microstructure and mechanical properties of SiCp / AZ61 magnesium metal matrix composites. J. Mater. Process. Tech. 272, 28–39 (2019). https://doi.org/10.1016/j.jmatprotec.2019.05.002
31. Singh, N., Agrawal, M.K., Saxena, K.K., Kumar, S., Prakash, C.: Advancement and influence of designing of ECAP on deformation and microstructure properties of the AA5083 under thermal effects. Int. J. Interact. Des. Manuf. 1–19 (2023)
32. Medeiros, M.P., Lopes, D.R., Kawasaki, M., Langdon, T.G., Figueiredo, R.B.: An Overview on the Effect of Severe Plastic Deformation on the Performance of Magnesium for Biomedical Applications. Materials (Basel). 16, 2401 (2023)
33. Kumar, H., Devade, K., Singh, D.P., Giri, J.M., Kumar, M., Arun, V.: Severe plastic deformation: A state of

 doi:10.20944/preprints202306.0173.v1

art. Mater. Today Proc. (2023)
34. Semenova, I.P., Modina, Y.M., Stotskiy, A.G., Polyakov, A.V., Pesin, M.V.: Fatigue Properties of Ti Alloys with an Ultrafine Grained Structure: Challenges and Achievements. Metals (Basel). 12, 312 (2022)
35. Sotniczuk, A., Kuczyńska-Zemła, D., Majchrowicz, K., Kijeńska-Gawrońska, E., Kruszewski, M., Nikiforow, K., Pisarek, M., Swieszkowski, W., Garbacz, H.: Tailoring mechanical and surface properties of UFG CP-Ti by the low-temperature annealing. Appl. Surf. Sci. 607, 155038 (2023)
36. Song, C., Liu, L., Deng, Z., Lei, H., Yuan, F., Yang, Y., Li, Y., Yu, J.: Research progress on the design and performance of porous titanium alloy bone implants. J. Mater. Res. Technol. (2023)
37. Shimizu, T., Fujibayashi, S., Yamaguchi, S., Yamamoto, K., Otsuki, B., Takemoto, M., Tsukanaka, M., Kizuki, T., Matsushita, T., Kokubo, T.: Bioactivity of sol–gel-derived TiO2 coating on polyetheretherketone: In vitro and in vivo studies. Acta Biomater. 35, 305–317 (2016)
38. Kaseem, M., Fatimah, S., Nashrah, N., Gun, Y.: Progress in Materials Science Recent progress in surface modification of metals coated by plasma electrolytic oxidation : Principle , structure , and performance. Prog. Mater. Sci. 117, 100735 (2021). https://doi.org/10.1016/j.pmatsci.2020.100735
39. Zakaria, A., Todoh, M., Jusoff, K.: Bio-Functional Coating on Ti6Al4V Surface Produced. (2020). https://doi.org/10.3390/met10091124
40. Costa, A.I., Gemini-Piperni, S., Alves, A.C., Costa, N.A., Checca, N.R., Leite, P.E., Rocha, L.A., Pinto, A.M.P., Toptan, F., Rossi, A.L.: TiO2 bioactive implant surfaces doped with specific amount of Sr modulate mineralization. Mater. Sci. Eng. C. 120, 111735 (2021)
41. Guo, T., Scimeca, J.-C., Ivanovski, S., Verron, E., Gulati, K.: Enhanced Corrosion Resistance and Local Therapy from Nano-Engineered Titanium Dental Implants. Pharmaceutics. 15, 315 (2023)
42. Amirabad, A.A., Johari, M., Parichehr, R., Aghdam, R.M., Dehghanian, C., Allahkaram, S.R.: Improving corrosion, antibacterial and biocompatibility properties of MAO-coated AZ31 magnesium alloy by Cu (II)-chitosan/PVA nanofibers post-treatment. Ceram. Int. (2023)
43. Makurat-Kasprolewicz, B., Ossowska, A.: Recent advances in electrochemically surface treated titanium and its alloys for biomedical applications: A review of anodic and plasma electrolytic oxidation methods. Mater. Today Commun. 105425 (2023)
44. Matos, A.O., Ricomini-Filho, A.P., Beline, T., Ogawa, E.S., Costa-Oliveira, B.E., de Almeida, A.B., Junior, F.H.N., Rangel, E.C., da Cruz, N.C., Sukotjo, C.: Three-species biofilm model onto plasma-treated titanium implant surface. Colloids Surfaces B Biointerfaces. 152, 354–366 (2017)
45. Wang, Y., Yu, H., Chen, C., Zhao, Z.: Review of the biocompatibility of micro-arc oxidation coated titanium alloys. Mater. Des. 85, 640–652 (2015)
46. Li, H., Wang, P., Wen, C.: Recent Progress on Nanocrystalline Metallic Materials for Biomedical Applications. Nanomaterials. 12, 2111 (2022)
47. Huvelle, L.: Superplasticity of a 3D-printed aluminium alloy, (2023)
48. Claudia, G.-M., Ivan, G., Laia, O.-M., Emilio, J.-P., Maria-Pau, G., Maurizio, V., Luís, C.J., Marta, P.: Influence of ECAP process on mechanical, corrosion and bacterial properties of Zn-2Ag alloy for wound closure devices. Mater. Des. 228, 111817 (2023)
49. Rzepa, S., Trojanová, Z., Džugan, J., Valiev, R.Z., Koukolíková, M., Melzer, D., Brázda, M.: Effect of ECAP processing on microstructure and mechanical behaviour of Ti-6Al-4V manufactured by directed energy deposition. Mater. Charact. 196, 112622 (2023)
50. Qadir, M., Li, Y., Munir, K., Wen, C.: Calcium phosphate-based composite coating by micro-arc oxidation (MAO) for biomedical application: a review. Crit. Rev. Solid State Mater. Sci. 43, 392–416 (2018)
51. Laino, L., La Noce, M., Fiorillo, L., Cervino, G., Nucci, L., Russo, D., Herford, A.S., Crimi, S., Bianchi, A., Biondi, A.: Dental pulp stem cells on implant surface: An in vitro study. Biomed Res. Int. 2021, (2021)
52. Zhang, W., Walboomers, X.F., van Kuppevelt, T.H., Daamen, W.F., Bian, Z., Jansen, J.A.: The performance of human dental pulp stem cells on different three-dimensional scaffold materials. Biomaterials. 27, 5658–5668 (2006)
53. Roy, M., Corti, A., Dominici, S., Pompella, A., Cerea, M., Chelucci, E., Dorocka-Bobkowska, B., Daniele, S.: Biocompatibility of Subperiosteal Dental Implants: Effects of Differently Treated Titanium Surfaces on the Expression of ECM-Related Genes in Gingival Fibroblasts. J. Funct. Biomater. 14, 59 (2023)
54. Atrens, A.: Understanding the Corrosion of Mg and Mg Alloys. Elsevier (2018)
55. Sunday, O., Fayomi, I., Akande, I.G., Popoola, A., Popoola, I., Molifi, H.: Potentiodynamic polarization studies of Cefadroxil and Dicloxacillin drugs on the corrosion susceptibility of aluminium AA6063 in 0 . 5

M nitric acid. Integr. Med. Res. 8, 3088–3096 (2019). https://doi.org/10.1016/j.jmrt.2018.12.028
56. Li, W., Gao, J., Ma, Y., Zheng, K., Zhi, J., Xin, Y., Xie, S., Yu, S.: Undoped and diamond-doped MAO coatings prepared on Ti6Al4V: Microstructure, wear, corrosion, and biocompatibility properties. Surf. Coatings Technol. 458, 129340 (2023)
57. Aun, D.P., Houmard, M., Mermoux, M., Latu-Romain, L., Joud, J.-C., Berthomé, G., Buono, V.T.L.: Development of a flexible nanocomposite TiO2 film as a protective coating for bioapplications of superelastic NiTi alloys. Appl. Surf. Sci. 375, 42–49 (2016)
58. Dehghanghadikolaei, A., Ibrahim, H., Amerinatanzi, A., Hashemi, M., Moghaddam, N.S., Elahinia, M.: Improving corrosion resistance of additively manufactured nickel–titanium biomedical devices by micro-arc oxidation process. J. Mater. Sci. 54, 7333–7355 (2019)
59. Wang, Y.-C., Lin, S.-H., Chien, C.-S., Kung, J.-C., Shih, C.-J.: In vitro bioactivity and antibacterial effects of a silver-containing mesoporous bioactive glass film on the surface of titanium implants. Int. J. Mol. Sci. 23, 9291 (2022)
60. Alipal, J., Saidin, S., Lo, A.Z.K., Koshy, P., Abdullah, H.Z., Idris, M.I., Lee, T.C.: In Vitro Surface Efficacy of CaP-based Anodised Titanium for Bone Implants. Surfaces and Interfaces. 102872 (2023)
61. Zhang, X., Zhang, T., Lv, Y., Zhang, Y., Lu, X., Xiao, J., Ma, C., Li, Z., Dong, Z.: Enhanced uniformity, corrosion resistance and biological performance of Cu-incorporated TiO2 coating produced by ultrasound-auxiliary micro-arc oxidation. Appl. Surf. Sci. 569, 150932 (2021)
62. Lin, Z., Wang, T., Yu, X., Sun, X., Yang, H.: Functionalization treatment of micro-arc oxidation coatings on magnesium alloys: A review. J. Alloys Compd. 879, 160453 (2021)
63. Du, Q., Wei, D., Wang, S., Cheng, S., Wang, Y., Li, B., Jia, D., Zhou, Y.: TEM analysis and in vitro and in vivo biological performance of the hydroxyapatite crystals rapidly formed on the modified microarc oxidation coating using microwave hydrothermal technique. Chem. Eng. J. 373, 1091–1110 (2019)
64. Wang, Y.-H., Liao, C.-C., Chen, Y.-C., Ou, S.-F., Chiu, C.-Y.: The feasibility of eco-friendly electrical discharge machining for surface modification of Ti: a comparison study in surface properties, bioactivity, and cytocompatibility. Mater. Sci. Eng. C. 108, 110192 (2020)
65. Grebņevs, V., Leśniak-Ziółkowska, K., Wala, M., Dulski, M., Altundal, Ş., Dutovs, A., Avotiņa, L., Erts, D., Viter, R., Vīksna, A.: Modification of physicochemical properties and bioactivity of oxide coatings formed on Ti substrates via plasma electrolytic oxidation in crystalline and amorphous calcium phosphate particle suspensions. Appl. Surf. Sci. 598, 153793 (2022)
66. Chang, C.-L., Huang, C.-H., Lin, C.-Y., Yang, F.-C., Tang, J.-F.: Mechanical properties of amorphous and crystalline CrN/CrAlSiN multilayer coating fabricated using HPPMS. Surfaces and Interfaces. 31, 102064 (2022)
67. Bignoli, F., Rashid, S., Rossi, E., Jaddi, S., Djemia, P., Terraneo, G., Bassi, A.L., Idrissi, H., Pardoen, T., Sebastiani, M.: Effect of annealing on mechanical properties and thermal stability of ZrCu/O nanocomposite amorphous films synthetized by pulsed laser deposition. Mater. Des. 221, 110972 (2022)
68. Buabthong, P., Ifkovits, Z.P., Kempler, P.A., Chen, Y., Nunez, P.D., Brunschwig, B.S., Papadantonakis, K.M., Lewis, N.S.: Failure modes of protection layers produced by atomic layer deposition of amorphous TiO 2 on GaAs anodes. Energy Environ. Sci. 13, 4269–4279 (2020)
69. Feng, Z., Hu, H., Wang, J., Dong, H., Zhang, X., Ma, J., Wang, J., Liu, D., Li, J., Zhang, X.: Revealing the evolution mechanisms of microstructure, texture and mechanical behavior in Zr702 alloy plates fabricated by accumulative roll bonding. Mater. Sci. Eng. A. 144609 (2023)
70. Chen, W.J., Xu, J., Liu, D.T., Shan, D. Bin, Guo, B., Langdon, T.G.: Thermal stability of ultrafine-grained pure titanium processed by high-pressure torsion. In: Materials Science Forum. pp. 338–344. Trans Tech Publ (2021)
71. Majchrowicz, K., Sotniczuk, A., Malicka, J., Choińska, E., Garbacz, H.: Thermal Stability and Mechanical Behavior of Ultrafine-Grained Titanium with Different Impurity Content. Materials (Basel). 16, 1339 (2023)
72. Zhang, G., Huang, S., Li, X., Zhao, D., Cao, Y., Liu, B., Huang, Q.: Oxide ceramic coatings with amorphous/nano-crystalline dual-structures prepared by micro-arc oxidation on Ti–Nb–Zr medium entropy alloy surfaces for biomedical applications. Ceram. Int. 49, 18114–18124 (2023)
73. Miyamoto, H.: Revealing What Enhance the Corrosion Resistance beside Grain Size in Ultrafine Grained Materials by Severe Plastic Deformation: Stainless Steels Case. Mater. Trans. MT-MF2022034 (2023)
74. Li, G., Ma, F., Liu, P., Qi, S., Li, W., Zhang, K., Chen, X.: Review of micro-arc oxidation of titanium alloys: Mechanism, properties and applications. J. Alloys Compd. 169773 (2023)

 doi:10.20944/preprints202306.0173.v1

75. Pandoleon, P., Bakopoulou, A., Papadopoulou, L., Koidis, P.: Evaluation of the biological behaviour of various dental implant abutment materials on attachment and viability of human gingival fibroblasts. Dent. Mater. 35, 1053–1063 (2019)